CLEAN
Soil Air Water

Rakesh Kumar Ghosh
D. Damodar Reddy

Division of Crop Chemistry and Soil Science, Central Tobacco Research Institute, Rajahmundry, Andhra Pradesh, India

Research Article

Crop Residue Ashes as Adsorbents for Basic Dye (Methylene Blue) Removal: Adsorption Kinetics and Dynamics

In the quest for identifying low-cost, locally available and effective adsorbents, pigeon pea (*Cajanus cajan* L.) residue ash (PRA) and sunflower (*Helianthus annuus* L.) residue ash (SRA) were evaluated as adsorbents for sequestering a basic dye, methylene blue (MB), from aqueous solution. Effects of contact time, initial solution pH and adsorbent dose on MB adsorption were investigated. MB adsorption onto PRA and SRA was dependent on initial solution pH, with adsorption being greater at higher pH. Percent MB removal increased with increase in adsorbent's dose. Adsorption followed pseudo-second order kinetics. Intraparticle diffusion was not the sole rate-controlling step. Both film diffusion and intraparticle diffusion controlled the adsorption process. The equilibrium data fitted well to Langmuir isotherm as compared to Freundlich isotherm, on the basis of coefficient of determination and error analysis. The maximum MB adsorption capacities of PRA and SRA were found as 58.8 and 62.5 $mg\,g^{-1}$, respectively. The free energy change and dimensionless equilibrium parameter revealed spontaneous and favorable nature of MB adsorption onto crop residue ashes. Results demonstrate that the PRA and SRA have high adsorptive potential as compared to many previously reported ash based adsorbents, and hence can be used for treating water contaminated with cationic dyes.

Keywords: Adsorption kinetics; Crop residue ash; Dye removal; Isotherm models

Received: May 15, 2013; *revised:* August 31, 2013; *accepted:* September 26, 2013

DOI: 10.1002/clen.201300386

1 Introduction

Industries such as textile, rubber, paper, leather, plastics, cosmetic, printing, etc., use a wide variety of synthetic dyes to produce a myriad of products to satisfy dynamic and ever evolving consumer's demand. About 5–10% of dyes used in these industries are, however, lost in industrial wastewater [1, 2]. Through the disposal of untreated dye-containing industrial wastewater to streams, dyes enter aquatic environments and pose a threat to the aquatic ecosystem not only by altering the physicochemical properties or biological activities of water [3], but also from toxicological stand point [4]. Through water bodies, dyes may gain entry to food chains and pose serious threat to human health [5, 6]. Proper treatment of dye-contaminated water is, therefore, an important issue for environment friendly disposal of stained wastewater.

As a result of extensive research work, a number of dye removal techniques such as adsorption, biosorption, biodegratation, electrochemical degradation, photochemical degradation, coagulation/flocculation, sonicated degradation, membrane filtration, etc., are available for treating stained wastewater [7]. Of all these techniques, dye removal through adsorption is most effective and practically feasible [8, 9]. Activated carbon is an undoubtedly effective adsorbent, but its high cost limits its large scale usage, particularly in developing countries. In order to circumvent these problems, there is a growing interest in the use of low-cost and easily available adsorbents, including various natural materials, wastes/by-products from agriculture or industry, for treatment of dye-contaminated wastewater [1, 10, 11]. However, not much research attention is paid to evaluate the potential of crop residue ash, the secondary by-product, as adsorbents to remove dye.

Crop residues are generated in huge quantities as a primary by-product of intensive agricultural production system. For example, in India about 523 Mt per annum crop residue is generated [12]. Crop residues of low lignocellulosic composition are used as a resource either in manure/compost preparation or as cattle feed. But, substantial quantities of high lignocellulosic residues of crops such as pigeon pea (9 Mt per annum in India) and sunflower (1 Mt per annum in India) are neither used for feeding cattle nor preparing manure [12]. Keeping these large volumes of high lignocellulosic crop residues in field often cause obstruction for agro-machinery/implements and also harbors pests. Burning of these crop residues, either in situ as farmer's common practice or off the field as fuels for thermal energy purposes generates a large quantity of crop residue ash, the secondary by-product, for which there is no alternative use.

Correspondence: Dr. R. Kumar Ghosh, Central Tobacco Research Institute, Rajahmundry 533105, Andhra Pradesh, India
E-mail: iarirakesh@gmail.com

Abbreviations: **FTIR**, Fourier transform IR; **MB**, Methylene blue; **OC**, organic carbon; **pH_{zpc}**, pH of zero point charge;; **PRA**, pigeon pea residue ash; **SRA**, sunflower residue ash; **TOC**, total OC

CLEAN Soil Air Water

The present study, therefore, aimed to evaluate pigeon pea (*Cajanus cajan* L.) stem residue ash (PRA) and sunflower (*Helianthus annuus* L.) stem residue ash (SRA) as adsorbents for methylene blue (MB) removal from aqueous solution. The effects of different process variables including contact time, initial solution pH, and adsorbent dose on adsorption of MB onto crop residue ashes were investigated. Different mathematical models namely pseudo-first order kinetic model, pseudo-second order kinetic model, and intraparticle diffusion model were tested to understand the kinetics, and mechanism of MB adsorption. Two isotherm models namely, Freundlich and Langmuir isotherm were investigated to evaluate the nature of adsorption equilibrium. Chi-square and percentage sum of error were calculated to analyze error and select the best fit mathematical model. The capacity and feasibility of MB adsorption onto PRA and SRA were also determined.

2 Materials and methods

2.1 Crop residue ashes

Pigeon pea and sunflower crop residues were collected from a local farmer's field near the Central Tobacco Research Institute, Rajahmundry, Andhra Pradesh. Crop residues were cleaned thoroughly to remove the surface adhered soil and dried. The dried crop residue stems (10 kg each for pigeon pea and sunflower) were burned in open air to simulate the practice followed by local farmers, i.e. burning of stems kept in heaps and it took about 30 min for complete burning, till weight of ash became constant. A 10 kg of pigeon pea and sunflower stem biomass reduced to 0.707 (92.93% weight loss) and 1.134 kg (88.66% weight loss), respectively, after burning and resulted in the ash that accounted for 7.07 and 11.34% of the stem biomass, respectively. The PRA and SRA so generated were passed through 1 mm sieve and stored in plastic containers.

2.2 Characterization of crop residue ashes

PRA and SRA were analyzed for organic carbon (OC) using a total organic carbon (TOC) analyzer (Elementar, Vario TOC select, Germany), pH (Systronics, Model 361, India), and electrical conductivity (EC) (Elico, Model CM 82T, India). The surface charge of crop residue ash was determined by measuring pH of zero point charge (pH_{zpc}) by potentiometric mass titration method [13]. Three doses (5, 7.5, and 10 g L^{-1}) of respective crop residue ash were agitated with 50 mL 0.03 M KNO_3 solution in a set of 150 mL Erlenmeyer flasks at 250 rpm for 24 h until the pH became constant. Then, 0.5 mL of 1 M KOH solution was added to each Erlenmeyer flask to deprotonate adsorbent's surface. The suspension was titrated by adding small volume of 0.1 M HNO_3 solution and pH was recorded after each addition, until pH of the suspension became constant. A similar procedure followed with 50 mL 0.03 M KNO_3 blank solution (without adsorbent). The potentiometric curves were drawn by plotting suspension's equilibrium pH values against the volume of 0.1 M HNO_3 added. The pH_{zpc} was determined from the intersection of the potentiometric curves with the blank. The functional groups of crop residue ashes were determined by Fourier transform IR (FTIR) spectrometry using attenuated total reflectance (ATR) (Bruker ALPHA, Germany). Samples were scanned (resolution 4 cm^{-1}) in the region of 4000–400 cm^{-1}. The specific surface area was calculated by Weng and Pan's [14] MB adsorption method which was reported to be in close agreement with that of the Brunauer–Emmet–Teller method.

2.3 MB

MB was selected as a model basic dye to explore the cationic dye adsorption behavior of crop residue ashes. Analytical grade MB (basic blue 9, molecular weight 373.91 g mol^{-1}) was used in the present study. MB stock solution of 1000 mg L^{-1} was prepared by dissolving 1 g MB in 1 L distilled water (pH 6.9), and subsequently working solutions of desired dye concentrations were prepared by serial dilution. The MB concentration in aqueous solution was determined by using UV–Vis spectrophotometry (Systronics, Model 2202, India) at a wavelength of maximum absorbance (λ_{max}) at 665 nm. Preliminary studies showed that initial pH (ranging from pH 2.08–11) of dye solution had no effect on the λ_{max} (665 nm) of MB, indicating stability of cationic MB within studied range of pH [15]. Therefore, a calibration curve prepared with distilled water (pH 6.9) was used in all adsorption experiments.

2.4 Batch adsorption experiments

2.4.1 Effect of process variables: Contact time, initial solution pH and adsorbent's dose

Adsorption kinetics was studied by agitating known amount of crop residue ash (0.5 g) with 50 mL MB solution of known concentration (50.4 mg L^{-1}) in a series of 150 mL Erlenmeyer flasks at 150 rpm over a period of 300 min. The sets of three flasks each were withdrawn at different time intervals (15, 30, 45, 60, 120, 180, 240, and 300 min). Kinetic studies were carried out at different initial pH values (2.08, 4.08, 6.02, and 7.91) of dye solution. The desired pH level of dye solution was obtained by adding either 0.1 M HCl or 0.1 M NaOH. The adsorbent-dye suspensions were centrifuged at 8000 rpm for 10 min and the MB concentration in supernatant estimated by measuring absorbance with UV–Vis spectrophotometry at 665 nm against the standard calibration curve. The amount of dye adsorbed at time t, q_t (mg g^{-1}) and dye removal percentage were calculated as:

$$q_t = \frac{(C_i - C_t)}{W} \quad (1)$$

$$\%\,\text{Removal} = \frac{100(C_i - C_t)}{C_i} \quad (2)$$

where C_i (mg L^{-1}) is initial MB concentration, C_t (mg L^{-1}) is MB concentration at time t (min), V is volume of the solution (L) and W is the mass of adsorbent (g).

The effect of adsorbent dose was investigated by equilibrating different quantities of crop residue ashes (2, 5, 10, 15, and 20 g L^{-1}) with 50 mL MB solution (pH 6.9) of known concentration (50.4 mg L^{-1}) at 150 rpm for 180 min. The MB concentration in the solution was determined as per the procedure detailed under kinetic study. All batch adsorption studies were carried out at room temperature ($27 \pm 1°C$).

2.4.2 Adsorption equilibrium experiments

Equilibrium experiments were performed by agitating 0.1 g of crop residue ash with 50 mL MB solution (pH 6.9) of different concentration (50.4, 108.4, 160.2, 183, 341, and 435 mg L^{-1}) in a set of 150 mL Erlenmeyer flasks at 150 rpm over a time period of 180 min. Samples

were centrifuged and MB concentrations in reaction mixtures were measured as described in Section 2.3. The amount of MB adsorbed (q_e) at equilibrium ($mg\,g^{-1}$) was calculated as follows:

$$q_e = \frac{(C_i - C_e)V}{W} \quad (3)$$

where C_e is the MB concentration in the solution at equilibrium ($mg\,L^{-1}$)and C_i, V, and W as previously defined.

All experiments were carried out in triplicate and relative standard deviation was calculated. Only mean values (with relative standard deviation <10%) are reported for ease of presentation. Adsorbate and adsorbent blanks were carried out simultaneously for all experiments as control to monitor interference.

2.5 Adsorption kinetics

Adsorption kinetics was investigated by fitting the kinetic data to pseudo-first order, pseudo-second order, and intraparticle diffusion model [7, 9, 16–18].

The pseudo-first order kinetic model can be expressed in linear form as:

$$\log(q_e - q_t) = \log(q_e) - \left(\frac{k_1}{2.303}\right)t \quad (4)$$

where q_e and q_t are the amount of dye adsorbed ($mg\,g^{-1}$) at equilibrium and time t (min), respectively. k_1 is the rate constant for the pseudo-first order model (min^{-1}), and it can be calculated from slope of the linear plot of $\log(q_e - q_t)$ against t.

The pseudo-second order kinetic model can be expressed in linear form as:

$$\frac{t}{q_t} = \left(\frac{1}{k_2 q_\alpha^2}\right) + \left(\frac{1}{q_\alpha}\right)t \quad (5)$$

where k_2 is the pseudo-second order rate constant ($g\,mg^{-1}\,min^{-1}$). q_e and k_2 can be calculated from the slope and intercept of the linear plot of t/q_t against t.

The kinetic data were further evaluated to understand the adsorption mechanism by intraparticle diffusion model, which can be linearly expressed as:

$$q_t = k_{id}t^{0.5} + C \quad (6)$$

where q_t ($mg\,g^{-1}$) is the amount adsorbed at time t (min), $t^{0.5}$ is the square root of the time (min), k_{id} ($mg\,g^{-1}\,min^{-0.5}$) is the intraparticle diffusion rate constant and C reflects boundary layer effect. k_{id} and C can be determined from the slope and intercept of the linear plot of q_t against $t^{0.5}$.

2.6 Adsorption isotherms

The adsorption equilibrium data were tested by two popularly used isotherm models namely, Freundlich and Langmuir isotherm [5, 15, 18, 19].

The linear form of Freundlich isotherm can be represented as:

$$\log(q_e) = \log(K_f) + \frac{1}{n}\log(C_e) \quad (7)$$

where q_e is the amount of dye adsorbed at equilibrium ($mg\,g^{-1}$), C_e is the dye concentration in solution at equilibrium ($mg\,L^{-1}$). K_f ($mg\,g^{-1}$) and $1/n$ are Freundlich constants, which indicate capacity and heterogeneity factor. K_f and $1/n$ can be calculated from the intercept and slope of the linear plot of $\log q_e$ against $\log C_e$.

The linear form of Langmuir isotherm can be represented as:

$$\frac{C_e}{q_e} = \frac{1}{kb} + \frac{C_e}{b} \quad (8)$$

where b is the Langmuir maximum adsorption capacity ($mg\,g^{-1}$) and k ($L\,mg^{-1}$) is the Langmuir bonding energy coefficient. k and b can be calculated from the intercept and slope of the linear plot of C_e/q_e against C_e.

The dimensionless separation factor/equilibrium parameter (R_L), an essential characteristic of Langmuir isotherm, was calculated as [7, 20]:

$$R_L = \frac{1}{(1 + kC_i)} \quad (9)$$

where, k ($L\,mg^{-1}$) is the Langmuir bonding energy coefficient and C_i is the highest initial dye concentration ($mg\,L^{-1}$). The value of R_L indicates the feasibility of dye adsorption. The value of R_L indicates either unfavorable ($R_L > 1$), linear ($R_L = 1$), favorable ($0 < R_L < 1$), or irreversible ($R_L = 0$) adsorption system.

The Gibb's free energy change (ΔG) of adsorption was estimated from the Langmuir binding energy constant k [21]. k ($L\,mg^{-1}$) was converted to K ($L\,mol^{-1}$) by using the molecular weight of MB before calculating the free energy change as:

$$\Delta G = -RT\ln(K) \quad (10)$$

where ΔG is free energy change of adsorption ($kJ\,mol^{-1}$), R is universal gas constant ($8.3145\,J\,mol^{-1}\,K^{-1}$), and T is temperature (K).

2.7 Analysis of error

Best-fit mathematical models were selected on the basis of error analysis. For this purpose, Chi-square (χ^2) and percent sum of error were calculated as:

$$\chi^2 = \frac{\sum (q_{e,exp} - q_{e,cal})^2}{q_{e,cal}} \quad (11)$$

$$\text{Sum of error}\,(\%) = \frac{100}{N-1}\sum \frac{(q_{e,exp} - q_{e,cal})}{q_{e,exp}} \quad (12)$$

where, $q_{e,exp}$ ($mg\,g^{-1}$) and $q_{e,cal}$ ($mg\,g^{-1}$) are the amount of dye adsorbed at equilibrium from experiment and mathematical model, respectively. N is the number of observations.

3 Results and discussion

3.1 PRA and SRA

Physicochemical analysis showed that organic carbon contents were 9.64 and 6.45% for PRA and SRA, respectively. The electrical conductivities of crop residue ashes were 6.73 and 10.98 $dS\,m^{-1}$ for PRA and SRA, respectively. Crop residue ashes were alkaline in nature

CLEAN Soil Air Water

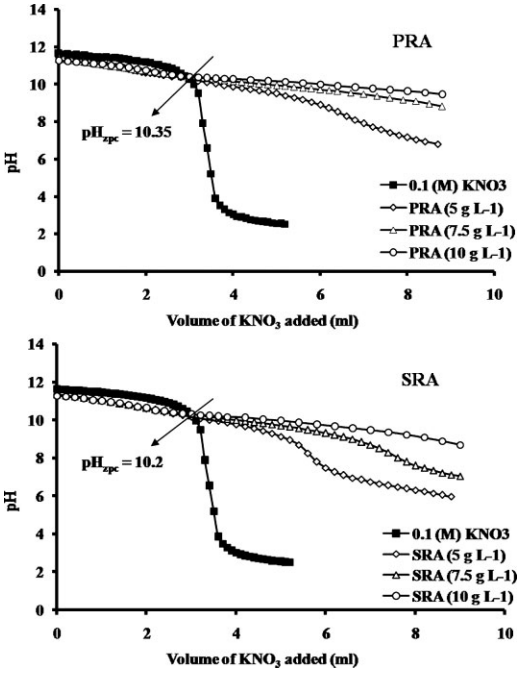

Figure 1. Zero point charge determination of PRA and SRA.

with pH values of 11.06 and 10.98 for PRA and SRA, respectively. Adsorbent's surface charge property was investigated by measuring the pH_{zpc} (Fig. 1). The pH_{zpc} of PRA and SRA were 10.35 and 10.2, respectively. Figure 2 depicts the FTIR spectrum of crop residue ashes. The FTIR analysis showed several bands, indicating presence of various functional groups, which could be helpful to understand the MB adsorption process. In both crop residue ashes, the band at 1045 cm^{-1}coupled with bands around 700–800 cm^{-1} represented SiO asymmetric and symmetric stretching vibrations, respectively. A prominent band at 1113 cm^{-1} with a small band at 641 cm^{-1} which corresponded to SiO_4^{4-} stretching vibrations were observed in SRA. Whereas, in PRA the 1113 cm^{-1} band was observed as a weak hump with 1045 cm^{-1} band which might be because of masking effect of the later band. Peaks in the area 500–650 cm^{-1} indicated silicate backbone of crop residue ashes. Both, PRA and SRA showed a strong band around1437 cm^{-1} with a band at 872 cm^{-1} and these represented asymmetric stretching and out-of-plane bending vibration of carbonate (CO_3^{2-}), respectively. These polar functional groups might play a significant role in the adsorption of cationic MB. Similar observations were reported for bagasse fly ash [15] and coal fly ash [22]. The specific surface area of PRA and SRA was 65.89 and 70.04 $m^2 g^{-1}$, respectively.

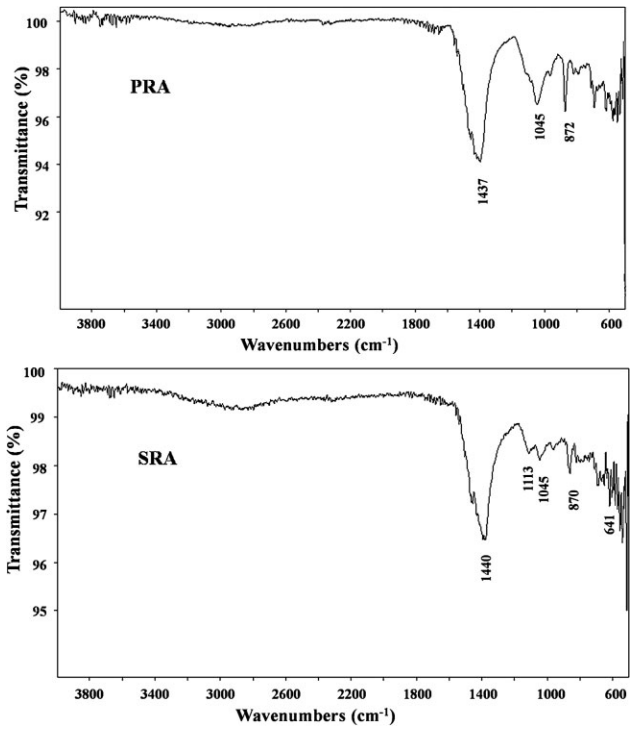

Figure 2. FTIR analysis of PRA and SRA.

3.2 Effect of contact time and initial solution pH on MB adsorption onto PRA and SRA

Figure 3 shows the effect of contact time and initial solution pH on MB adsorption onto known amount of crop residue ash from MB

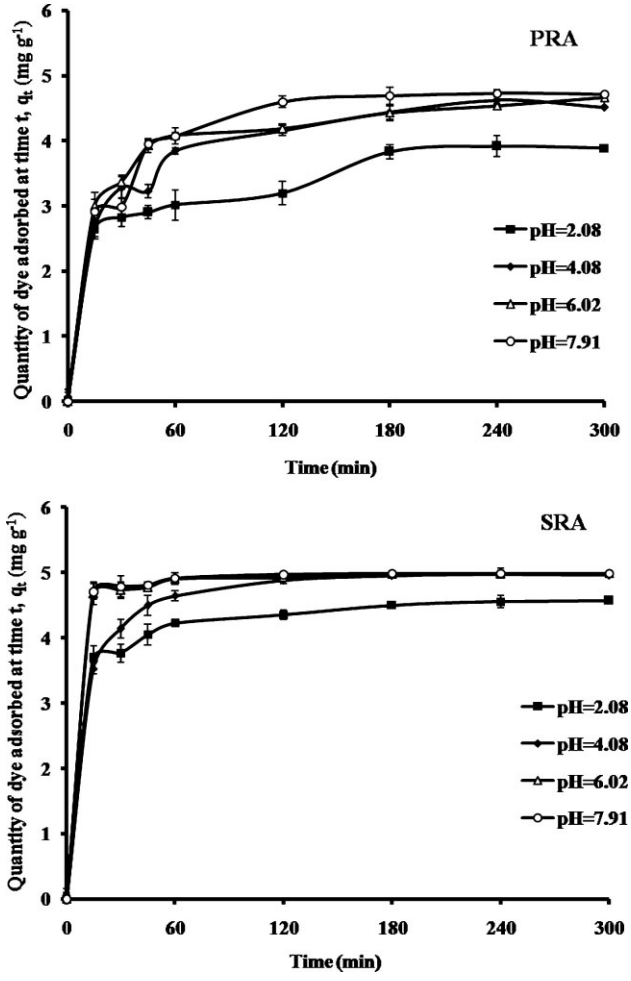

Figure 3. Effect of contact time and initial solution pH on MB adsorption onto PRA and SRA, experimental conditions: volume of dye solution = 50 mL, crop residue ash dosage = 0.5 g, initial dye concentration = 50.4 mg L^{-1}, temperature = 27 ± 1°C, shaker speed = 150 rpm.

solution of known concentration (50.4 mg L^{-1}). The results indicated that MB adsorption varied slightly between PRA and SRA, but showed consistent increase with contact time and rise in initial solution pH. It is very clear that MB adsorption was fast at the initial stage of adsorption. The amount of MB adsorbed per unit mass of adsorbent (q_t) reached to 2.65–2.92 mg g^{-1} (52–58% of MB solution concentration) for PRA and 3.67–4.71 mg g^{-1} (73–93% of MB solution concentration) for SRA within 15 min of adsorption. The reason could be that, initially adsorption sites of adsorbent were vacant, and the moment they came in contact with the MB solution, MB molecules diffused at a very fast rate from bulk dye solution to the adsorption sites [14, 23, 24]. Subsequently the rate of adsorption decreased with increase in time, and after 180 min there was no change in the q_t values, leading to the state of equilibrium. Figure 3 also shows that though the amount of MB adsorbed per unit mass of adsorbent (q_t) were different for solution of different initial pH values, the reaction matrix attained state of equilibrium within 180 min in all cases. Thus, 180 min was selected as a time for attaining equilibrium state of MB adsorption onto PRA and SRA in all other batch adsorption experiments.

The pH plays a significant role in adsorption of dye onto adsorbent's surface by influencing the ionization of dye molecule and charge intensity of adsorbent surface [7, 23, 24]. Figure 3 depicts that, at any particular time, MB adsorption (q_t) onto crop residue ashes increased with increase in initial solution pH and maximum adsorption was observed at the alkaline pH 7.91. For example, at equilibrium time of 180 min, MB adsorption (q_t) increased from 3.83 to 4.69 mg g^{-1} for PRA and 4.5 to 4.97 mg g^{-1} for SRA with rise in initial solution pH from 2.08 to 7.91 (Fig. 4). In aqueous phase, MB exists as a cation and gets adsorbed onto adsorbent's negatively charged sites because of electrostatic attraction. Low adsorption of MB at acidic pH (2.08) is due to decrease in the negative charge density on the adsorbent's surface at acidic pH as a result of protonation, coupled with the competition between H^+ ions and cationic MB molecules for the same negatively charged sites of adsorbent. MB adsorption increased with increase in initial solution pH $\geq$ 4.08 (Fig. 4). For the initial solution with pH $\geq$ 4.08, the pH of equilibrium solution was greater than the pH_{zpc} values SRA (10.2) and PRA (10.35). When the pH of the system was higher than the pH_{zpc} of adsorbent, the sorbent's surface negative charge density increased, and resulted in high MB sequestration. Similar observations were noticed on other ashes like sludge ash [14] and rice husk ash [23].

3.3 Effect of crop residue ash dose

Figure 5 represents the effect of dose of crop residue ashes (PRA and SRA) on MB sequestration from a fixed volume MB solution of known dye concentration (50.4 mg L^{-1}). The results showed that MB removal increased from 50.6 to 94.1% for PRA and 56.6 to 97.2% for SRA with increased adsorbent's dose from 2 to 10 g L^{-1}, and thereafter, the percentage MB removal remained unchanged. However, the amount of MB adsorbed per unit mass of adsorbent (q_t) decreased from 10.74 to 2.55 mg g^{-1} for PRA and 12.04 to 2.6 mg g^{-1} for SRA with increase in adsorbent's dose from 2 to 20 g L^{-1}. For a fixed volume of dye solution with known initial dye concentration, the total amount of dye present in the solution also becomes constant. Adsorbent's dose is of prime importance because a fixed amount of adsorbent has fixed number of binding sites, and it can only adsorb a fixed mass of dye. Thus, with increase in adsorbent dose, the number of adsorbing sites increases and results in higher percentage dye removal [5, 9]. Selecting effective dose of adsorbent for efficient and economic removal of dye had always been a focus of dosage study [8]. Thus, by considering >94% of dye removal, crop residue ash dose of 10 g L^{-1} was selected as an optimum dose for batch adsorption studies.

3.4 Adsorption kinetics

The pseudo-first order and pseudo-second order models were used to understand the kinetic nature of crop residue ash–MB sorption system (Tab. 1). Table 1 clearly shows that $q_{e,exp}$ values were not in agreement with $q_{e,cal}$ values from pseudo-first order kinetic model with relatively low coefficient of determination (R^2 = 0.814–0.979). In contrast, the $q_{e,cal}$ values from pseudo-second order kinetic model were in good agreement with $q_{e,exp}$ values and had high coefficient of determination (R^2 = 0.989–0.999). These results indicated that the pseudo-second order model described MB adsorption kinetics better

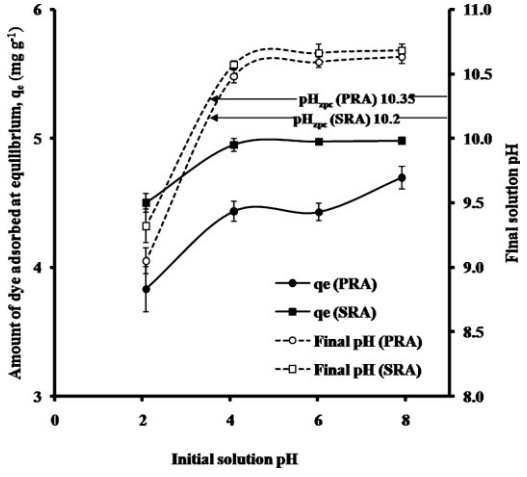

Figure 4. Effect of initial solution pH on MB adsorption onto PRA and SRA and final pH of solution, experimental conditions: volume of dye solution = 50 mL, crop residue ash dosage = 0.5 g, initial dye concentration = 50.4 mg L^{-1}, temperature = 27 ± 1°C, shaker speed = 150 rpm.

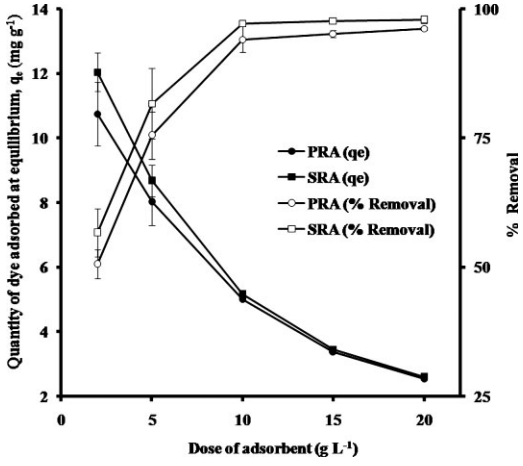

Figure 5. Effect of adsorbent dose on the adsorption of MB onto PRA and SRA, experimental conditions: volume of dye solution = 50 mL, initial dye concentration = 50.4 mg L^{-1}, temperature = 27 ± 1°C, pH 6.9, shaker speed = 150 rpm.

CLEAN Soil Air Water

Table 1. Kinetic parameters for adsorption of methylene blue onto PRA and SRA

			Kinetic model							
			Pseudo-first-order			Pseudo-second order			Intraparticle diffusion	
Adsorbent	pH	$q_{e,exp}$ (mg g^{-1})	k_1 (min^{-1})	R^2	$q_{e,cal}$ (mg g^{-1})	k_2 (g mg^{-1} min^{-1})	R^2	$q_{e,cal}$ (mg g^{-1})	C (mg g^{-1})	R^2
PRA	2.08	3.83	0.005	0.961	1.21	0.014	0.994	4.12	2.17	0.919
	4.08	4.44	0.016	0.945	2.15	0.013	0.998	4.83	2.18	0.919
	6.02	4.43	0.016	0.814	1.41	0.018	0.999	4.78	2.26	0.819
	7.91	4.69	0.028	0.979	3.19	0.015	0.998	4.97	2.73	0.855
SRA	2.08	4.50	0.016	0.929	1.01	0.034	0.999	4.67	3.39	0.910
	4.08	4.95	0.023	0.975	1.73	0.033	0.999	5.10	3.37	0.798
	6.02	4.98	0.028	0.977	2.07	0.153	0.999	5.02	4.57	0.893
	7.91	4.97	0.016	0.841	2.59	0.121	0.998	5.03	4.62	0.880

than the pseudo-first order kinetic model. The pseudo-second order rate constant (k_2) values of MB adsorption were 2.4–8.5 times higher for SRA than that for PRA. The higher $k_2$values implied greater MB adsorption onto SRA than PRA. Similarly, the pseudo-second order kinetic model was reported best for several other adsorbents like rice hull ash [20], H_2SO_4 treated fly ash [25], etc.

3.5 Adsorption mechanism

To understand the adsorption mechanism, determination of rate limiting stage has always been a point of interest in adsorption studies. Reported literature showed that transfer of dye molecules from the bulk solution to the sorbent surface is either by boundary layer/film diffusion or by intraparticle diffusion or by both [18, 24]. To investigate the mechanism involved in MB adsorption onto PRA and SRA, experimental kinetic data were tested with the intraparticle diffusion model (Tab. 1 and Fig. 6). Figure 6 shows that adsorption plots were not linear over the whole time frame, indicating multi-stage adsorption [20, 26]. The intraparticle diffusion rate constant (k_{id}) and C (boundary layer thickness) were determined from the slope and intercept of the linear regression line of q_t against $t^{0.5}$. If the regression line of q_t against $t^{0.5}$ is linear and passes through the origin ($C = 0$), then intraparticle diffusion is the sole rate-limiting step. Table 1 shows that the regression lines for intraparticle diffusion model had good coefficient of determination ($R^2 = 0.81$–0.92), which indicated suitability of the model. But, the regression lines did not pass through the origin ($C \neq 0$) and had intercepts (C values in Tab. 1 and Fig. 6), thereby indicating that though intraparticle diffusion was involved, but it was not the only mechanism. Fast adsorption in the initial stages could be controlled by film diffusion, while the slow adsorption at the later stages could be mainly governed by intraparticle diffusions [7, 18]. The C values for SRA were higher than that for PRA, which indicated greater boundary layer effect for SRA-MB adsorption systems as compared to that of PRA-MB adsorption systems. It is very clear from Tab. 1 that C values (boundary layer effect) increased with increase in initial solution pH for each crop residue ash and consequently resulted in higher MB adsorption at increased pH.

3.6 Adsorption isotherms

The dynamics of MB adsorption onto PRA and SRA was explained by unfolding the adsorption equilibrium data. Equilibrium data were tested with Freundlich and Langmuir isotherm [15, 19]. Figure 7 shows Freundlich and Langmuir isotherm fitting for PRA and SRA. The isotherm parameters are described in Tab. 2. On the basis of coefficient of determination (R^2), both Freundlich ($R^2 = 0.978$–0.989) and Langmuir ($R^2 = 0.996$–0.992) isotherms were able to describe the equilibrium adsorption (Tab. 2). However, because of small differences in R^2 values, the best-fit isotherm model was selected on the basis of error analysis. The $q_{e,exp}$ values and $q_{e,cal}$ values from isotherm models were evaluated by Chi-square and sum of error (%). The values of Chi-square and

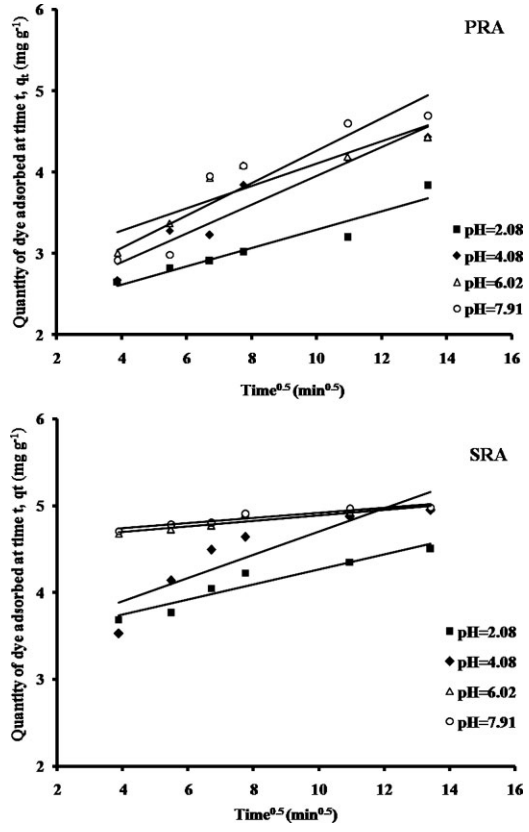

Figure 6. Intraparticle diffusion model for MB adsorption onto PRA and SRA, experimental conditions: volume of dye solution = 50 mL, crop residue ash dosage = 0.5 g, initial dye concentration = 50.4 mg L^{-1}, temperature = 27 ± 1°C, shaker speed = 150 rpm.

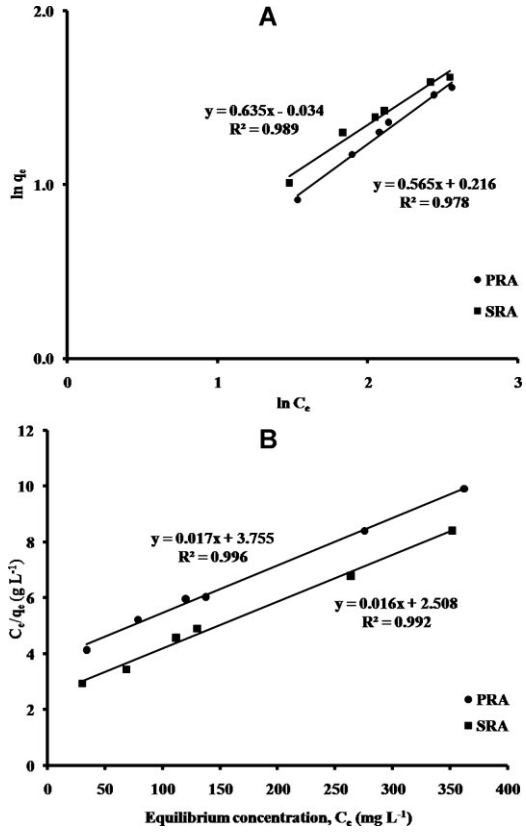

Figure 7. (A) Freundlich and (B) Langmuir isotherms for MB adsorption onto PRA and SRA, experimental conditions: volume of dye solution = 50 mL, crop residue ash dosage = 0.1 g, initial dye concentrations = 50.4, 108.4, 160.2, 183, 341, and 435 mg L^{-1}, temperature = 27 ± 1°C, shaker speed = 150 rpm.

Table 2. Adsorption isotherm parameters for adsorption of methylene blue onto PRA and SRA

Mathematical model	Parameter	PRA	SRA
Freundlich isotherm	K_f (mg g^{-1})	1.08	1.64
	$1/n$	0.635	0.565
	R^2	0.989	0.978
	χ^2	0.351	0.617
	SE (%)	5.10	7.05
Langmuir isotherm	b (mg g^{-1})	58.8	62.5
	k (L mg^{-1})	0.004	0.006
	R^2	0.996	0.992
	R_L	0.337	0.265
	χ^2	0.046	0.319
	SE (%)	2.25	4.85

SE, sum of error.

sum of error (%) for Freundlich and Langmuir isotherms are presented in Tab. 2. The results showed that Chi-square and sum of error (%) values were lower for Langmuir isotherm as compared to that of Freundlich isotherm. Thus, Langmuir isotherm was found to best explain the MB adsorption onto PRA and SRA. The monolayer adsorption capacity of PRA and SRA was 58.8 and 62.5 mg g^{-1}, respectively. The value of dimensionless separation factor (R_L) at highest initial dye concentration for MB adsorption onto PRA and SRA were 0.337 and 0.265, respectively, which indicated favorable ($0 < R_L < 1$) conditions for MB adsorption onto crop residue ashes [17]. Comparatively lower value of R_L for SRA than that for PRA explained relatively more favorable sequestration of MB by SRA. The ΔG values were −1.31 and −2.17 kJ mol^{-1} for MB adsorption onto PRA and SRA, respectively, at room temperature (27 ± 1°C). The negative values of ΔG indicated that the MB adsorption onto crop residue ashes was a spontaneous and favorable process.

Table 3. Comparison of methylene blue adsorption capacities of different ash based absorbents

Adsorbent	pH	Contact time	Adsorption capacity (mg g^{-1})	Reference
Coconut bunch waste	6.5–7.5	315 min	70.9	[21]
Yellow passion fruit	8.0	48 h	44.7	[27]
Oak sawdust	–	270 min	38.5	[5]
Sugarcane bagasse	5.8	240 h	34.2	[28]
Orange peel	7.2	24 h	18.6	[29]
Blast furnace sludge	6.5–7.0	120 min	6.4	[30]
Neem sawdust	7.2	30 min	3.6	[31]
Bagasse fly ash	8.0	24 h	75.5	[15]
Rice hull ash	–	150 min	50.5	[20]
Tobacco stem ash	6.9	180 min	35.7	[32]
Salvadorapersica stem ash	11.0	80 min	22.8	[19]
Rice husk ash	7.2	60 min	6.9	[33]
Fly ash (sonochemical treated)	9.4	–	4.5	[34]
Bio-sludge ash	9.83	72 h	1.9	[14]
Fly ash (H_2SO_4 treated)	–	72 h	0.8	[25]
PRA	6.9	180 min	58.2	Present study
SRA	6.9	180 min	62.5	Present study

3.7 Comparison of crop residue ashes with reported adsorbents

The MB adsorption capacities of crop residue ashes, PRA and SRA, were compared with some other previously reported non-ash and ash based adsorbents (Tab. 3). The crop residue ashes, PRA and SRA, were found to be superior to many reported adsorbents.

4 Concluding remarks

Removal of MB from aqueous solution by crop residue ashes (PRA and SRA) had been investigated. MB adsorption kinetics was best explained by pseudo-second order model. Intraparticle diffusion was not sole rate controlling step, and boundary layer diffusion increased with increasing solution pH. MB adsorption equilibrium on the duo ashes, PRA and SRA, was best explained by Langmuir isotherm, with maximum MB adsorption capacities of 58.8 and 62.5 mg g^{-1} for PRA and SRA, respectively. The Langmuir equilibrium parameter (R_L) and Gibb's free energy change indicated favorable and spontaneous adsorption of MB adsorption onto PRA and SRA. The results of the present study demonstrated that the PRA and SRA had high adsorptive potential as compared to many previously reported ash based adsorbents, and hence could be used for treating cationic dye-contaminated water.

Acknowledgments

The authors wish to thank the Director, CTRI, for extending all facilities required for this research, and the technical staff of CC & SS Division, CTRI, for their assistance throughout the course of this study.

The authors have declared no conflict of interest.

References

[1] V. K. Gupta, Suhas, Application of Low Cost Adsorbents for Dye Removal – a Review, *J. Environ. Manage.* **2009**, *90*, 2313–2342.

[2] Y. Liu, J. Wang, Y. Zheng, A. Wang, Adsorption of Methylene Blue by Kapok Fiber Treated by Sodium Chlorite Optimized with Response Surface Methodology, *Chem. Eng. J.* **2012**, *184*, 248–255.

[3] J. G. Montano, F. Torrades, L. A. Perez Estrada, I. Oller, S. Malato, M. I. Maldonado, J. Peral, Degradation Pathways of the Commercial Reactive Azo Dye Procion Red H-E7B under Solar-Assisted Photo-Fenton Reaction, *Environ. Sci. Technol.* **2008**, *42*, 6663–6670.

[4] I. A. W. Tan, B. H. Hameed, A. L. Ahmad, Equilibrium and Kinetic Studies on Basic Dye Adsorption by Oil Palm Fibre Activated Carbon, *Chem. Eng. J.* **2007**, *127*, 111–119.

[5] M. M. Abd EI-Latif, A. M. Ibrahim, M. F. El-Kady, Adsorption Equilibrium, Kinetics and Thermodynamics of Methylene Blue from Aqueous Solutions Using Biopolymer Oak Sawdust Composite, *J. Am. Sci.* **2010**, *6* (*6*), 267–283.

[6] P. Saha, S. Datta, Assessment on Thermodynamics and Kinetics Parameters on Reduction of Methylene Blue Dye Using Flyash, *Desalin. Water Treat.* **2009**, *12*, 219–228.

[7] M. C. Somasekhara Reddy, L. Sivaramakrishna, A. Varada Reddy, The Use of an Agricultural Waste Material, Jujuba Seeds for the Removal of Anionic Dye (Congo Red) from Aqueous Medium, *J. Hazard. Mater.* **2012**, *203–204*, 118–127.

[8] M. A. M. Salleh, D. K. Mahmoud, W. A. Karim, A. Idris, Cationic and Anionic Dye Adsorption by Agricultural Solid Wastes: A Comprehensive Review, *Desalination* **2011**, *280* (*1–3*), 1–13.

[9] Y. Feng, H. Zhou, G. Liu, J. Qiao, J. Wanga, H. Lu, L. Yang, Y. Wua, Methylene Blue Adsorption onto Swede Rape Straw (*Brassica napus* L.) Modified by Tartaric Acid: Equilibrium, Kinetic and Adsorption Mechanisms, *Bioresour. Technol.* **2012**, *125*, 138–144.

[10] H. Parab, M. Sudersanan, N. Shenoy, T. Pathare, B. Vaze, Use of Agro-Industrial Wastes for Removal of Basic Dyes from Aqueous Solutions, *Clean – Soil Air Water* **2009**, *37* (*12*), 963–969.

[11] M. Rafatullah, O. Sulaiman, R. Hashim, A. Ahmad, Adsorption of Methylene Blue on Low Cost Adsorbents – a Review, *J. Hazard. Mater.* **2010**, *177*, 70–80.

[12] B. S. Pathak, Crop Residues to Energy, *Environ. Agric.* **2006**, *7*, 854–869.

[13] N. Fiol, I. Villaescusa, Determination of Sorbent Point Zero Charge: Usefulness in Sorption Studies, *Environ. Chem. Lett.* **2009**, *7*, 79–84.

[14] C. H. Weng, Y. F. Pan, Adsorption Characteristics of Methylene Blue from Aqueous Solution by Sludge Ash, *Colloid. Surf., A* **2006**, *274* (*1*), 154–162.

[15] V. K. Gupta, D. Mohan, S. Sharma, M. Sharma, Removal of Basic Dyes (Rhodamine B and Methylene Blue) from Aqueous Solutions Using Bagasse Fly Ash, *Sep. Sci. Technol.* **2000**, *35* (*13*), 2097–2113.

[16] Y. S. Ho, G. McKay, Sorption of Dye from Aqueous Solution by Peat, *Chem. Eng. J.* **1998**, *70* (*2*), 115–124.

[17] Y. S. Ho, G. McKay, Pseudo-Second Order Model for Sorption Processes, *Process Biochem.* **1999**, *34* (*5*), 451–465.

[18] B. H. Hameed, D. K. Mahmoud, A. L. Ahmad, Equilibrium Modeling and Kinetic Studies on the Adsorption of Basic Dye by a Low-Cost Adsorbent: Coconut (*Cocos nucifera*) Bunch Waste, *J. Hazard. Mater.* **2008**, *158*, 65–72.

[19] E. Bazrafshan, F. Mostafapour, M. A. Zazouli, Methylene Blue (Cationic Dye) Adsorption into *Salvadora persica* Stems Ash, *Afr. J. Biotechnol.* **2012**, *11* (*101*), 16661–16668.

[20] X. G. Chen, S. S. Lv, S. T. Liu, P. P. Zhang, A. B. Zhang, J. Sun, Y. Ye, Adsorption of Methylene Blue by Rice Hull Ash, *Sep. Sci. Technol.* **2012**, *47* (*1*), 147–156.

[21] P. Leechart, W. Nakbanpote, P. Thiravetyan, Application of 'Waste' Wood-Shaving Bottom Ash for Adsorption of Azo Reactive Dye, *J. Environ. Manage.* **2009**, *90*, 912–920.

[22] A. Sarkar, R. Rano, G. Udaybhanu, A. K. Basu, A Comprehensive Characterization of Fly Ash from a Thermal Power Plant in Eastern India, *Fuel Process. Technol.* **2006**, *87*, 259–277.

[23] A. K. Chowdhury, A. D. Sarkar, A. Bandyopadhyay, Rice Husk Ash as a Low Cost Adsorbent for the Removal of Methylene Blue and Congo Red in Aqueous Phases, *Clean – Soil Air Water* **2009**, *37* (*7*), 581–591.

[24] M. T. Yagub, T. K. Sen, H. M. Ang, Equilibrium, Kinetics, and Thermodynamics of Methylene Blue Adsorption by Pine Tree Leaves, *Water Air Soil Pollut.* **2012**, *223* (*8*), 5267–5282.

[25] J. X. Lin, S. L. Zhan, M. H. Fang, X. Q. Qian, H. Yang, Adsorption of Basic Dye from Aqueous Solution onto Fly Ash, *J. Environ. Manage.* **2008**, *87*, 193–200.

[26] D. Kavitha, C. Namasivayam, Experimental and Kinetic Studies on Methylene Blue Adsorption by Coir Pith Carbon, *Bioresour. Technol.* **2007**, *98*, 14–21.

[27] F. A. Pavan, E. C. Lima, S. L. P. Dias, A. C. Mazzocato, Methylene Blue Biosorption from Aqueous Solutions by Yellow Passion Fruit Waste, *J. Hazard. Mater.* **2008**, *150*, 703–712.

[28] N. C. Filho, E. C. Venancio, M. F. Barriquello, A. A. Hechenleitner, E. A. G. Pineda, Methylene Blue Adsorption onto Modified Lignin from Sugarcane Baggasse, *Ecletica Quím.* **2007**, *32* (*4*), 63–70.

[29] G. Annadurai, R. S. Juang, D. J. Lee, Use of Cellulose-Based Wastes for Adsorption of Dyes from Aqueous Solutions, *J. Hazard. Mater.* **2002**, *B92* (*3*), 263–274.

[30] A. K. Jain, V. K. Gupta, A. Bhatnagar, S. Jain, Suhas, A Comparative Assessment of Adsorbents Prepared from Industrial Wastes for the Removal of Cationic Dye, *J. Indian Chem. Soc.* **2003**, *80*, 267–270.

[31] S. D. Khattri, M. K. Singh, Colour Removal from Synthetic Dye Wastewater Using a Bioadsorbent, *Water Air Soil Pollut.* **2000**, *120*, 283–294.

[32] R. K. Ghosh, D. D. Reddy, Tobacco Stem Ash as an Adsorbent for Removal of Methylene Blue from Aqueous Solution: Equilibrium, Kinetics and Mechanism of Adsorption, *Water Air Soil Pollut.* **2013**, *224* (*6*), 1582.

[33] D. Sarkar, A. Bandyopadhyay, Adsorptive Mass Transport of Dye on Rice Husk Ash, *J. Water Resour. Prot.* **2010**, *2*, 424–431.

[34] S. Wang, Z. H. Zhu, Sonochemical Treatment of Fly Ash for Dye Removal from Wastewater, *J. Hazard. Mater.* **2005**, *126* (*1–3*), 91–95.

